available at www.sciencedirect.com

SCIENCE DIRECT®

www.elsevier.com/locate/brainres

BRAIN RESEARCH

Research Report

Specialization of pyramidal cell structure in the visual areas V1, V2 and V3 of the South American rodent, *Dasyprocta primnolopha*

Guy N. Elston[a,*], *Alejandra Elston*[a], *Marco Aurelio-Freire*[b], *Wallace Gomes Leal*[b], *Ivanira Amaral Dias*[b], *Antonio Pereira Jr.*[c], *Luiz Carlos L. Silveira*[c], *Cristovam W. Picanço Diniz*[b]

[a]*Vision, Touch and Hearing Research Centre, School of Biomedical Sciences, The University of Queensland, Queensland, 4072, Australia*
[b]*Laboratório de Neuroanatomia Funcional, Departamento de Morfologia, Centro de Ciências Biológicas, Universidade Federal do Pará, 66075-900 Belém, Pará, Brazil*
[c]*Departamento de Fisiologia, Centro de Ciências Biológicas, Universidade Federal do Pará, 66075-900 Belém, Pará, Brazil*

ARTICLE INFO

Article history:
Accepted 17 May 2006
Available online 18 July 2006?>

Keywords:
Striate
Extrastriate
Dendrite
Spine
Lucifer yellow
Rat
Monkey

ABSTRACT

Marked phenotypic variation has been reported in pyramidal cells in the primate cerebral cortex. These extent and systematic nature of these specializations suggest that they are important for specialized aspects of cortical processing. However, it remains unknown as to whether regional variations in the pyramidal cell phenotype are unique to primates or if they are widespread amongst mammalian species. In the present study we determined the receptive fields of neurons in striate and extrastriate visual cortex, and quantified pyramidal cell structure in these cortical regions, in the diurnal, large-brained, South American rodent *Dasyprocta primnolopha*. We found evidence for a first, second and third visual area (V1, V2 and V3, respectively) forming a lateral progression from the occipital pole to the temporal pole. Pyramidal cell structure became increasingly more complex through these areas, suggesting that regional specialization in pyramidal cell phenotype is not restricted to primates. However, cells in V1, V2 and V3 of the agouti were considerably more spinous than their counterparts in primates, suggesting different evolutionary and developmental influences may act on cortical microcircuitry in rodents and primates.

1. Introduction

Studies in primates have revealed marked differences in pyramidal cell structure among different cortical regions (Lund et al., 1993; Elston et al., 1999a, 2005a; Elston, 2000; Elston and Rockland, 2002; Jacobs et al., 2001). Moreover, cell/circuit structure differs systematically in functionally related cortical areas such that more complex cells/circuits perform more complex functions. For example, pyramidal cells become more complex with anterior progression

* *Corresponding author*. Fax: +61 7 33654522.
E-mail address: G.Elston@vthrc.uq.edu.au (G.N. Elston).

0006-8993/$ – see front matter © 2006 Elsevier B.V. All rights reserved.
doi:10.1016/j.brainres.2006.05.100

from the primary visual to second visual areas and those of the temporal and parietal lobes (Elston, 2003c; Elston and Rosa, 1997, 1998, in press; Elston et al., 1999b, 2005b, d,g). Likewise, pyramidal cells become progressively more complex with progression from the primary somatosensory cortex to sensory association areas (Elston and Rockland, 2002; Elston et al., 2005c,e). The systematic nature of these structural specializations is believed to subserve global cortical functions (see Elston, 2002, 2003b, in press; Elston and Zietsch, 2005; Jacobs and Scheibel, 2002 for reviews). However, it is not yet known whether pyramidal cell structure varies systematically between functionally related cortical areas in other mammalian species, particularly those with smaller lissencephalic cortices with fewer cortical areas.

Recent data sampled from rats and mice suggest that pyramidal cells in their cortices are considerably less heterogeneous than reported in primates (Elston et al., 1997; Dierssen et al., 2002; Benavides-Piccione et al., 2005, 2006; Ballesteros-Yáñez et al., 2006), but relatively few cortical areas have been included for study. Moreover, present controversy regarding the organization of visual cortex in these rodents (Sereno et al., 1994; Rosa and Krubitzer, 1999), and the relatively small size of their brains, makes it difficult to inject sufficient numbers of pyramidal cells among visual areas to allow meaningful statistical comparisons. Thus it remains to be determined how phylogeny, development and laws of form may influence specializations in the pyramidal cell phenotype.

Here we mapped visual response properties in striate and extrastriate cortical areas of the large diurnal rodent, the agouti (*Dasyprocta primnolopha*), and injected large numbers of pyramidal cells to allow further basis for comparison. This species was selected as it is a visual forager, has a relatively large brain and has a relatively large, easily identifiable primary visual area (Picanço Diniz, 1987; Picanço-Diniz et al., 1989). Our mapping studies revealed a continuous belt of visual cortex adjacent and lateral to the primary visual area (V1), which contained a complete map of visual space. Receptive field reversals were noted with lateral progression from V1 through this region. In addition, this belt was distinguished from V1 by cyto- and myeloarchitecture. We named this region the second visual area (V2), consistent with other species. Lateral to and continuous with V2 we found neurons responsive to visual stimuli in both the vertical and horizontal meridians. The location of this region and the size of the receptive fields of neurons contained within suggest this region includes the third visual area (V3, or V3 complex). Visually responsive neurons were also found lateral to V3, and we have tentatively named this region the posterior temporal area (TP). We then injected large numbers of pyramidal cells in layer III of V1, V2 and V3 for comparison. We found marked and systematic differences in pyramidal cell structure among these visual areas. Those in V1 were smaller and less spinous than those in V2, which were smaller and less spinous than those in V3. The trend for a systematic increase in the morphological complexity of pyramidal cells in visual cortex reported here parallels that observed in simian and prosimian primates, but differs to that reported in the tree shrew. Notably, cells in V1, V2 and V3 of the agouti are considerably more spinous than those in homologous cortical areas in primates (Fig. 1).

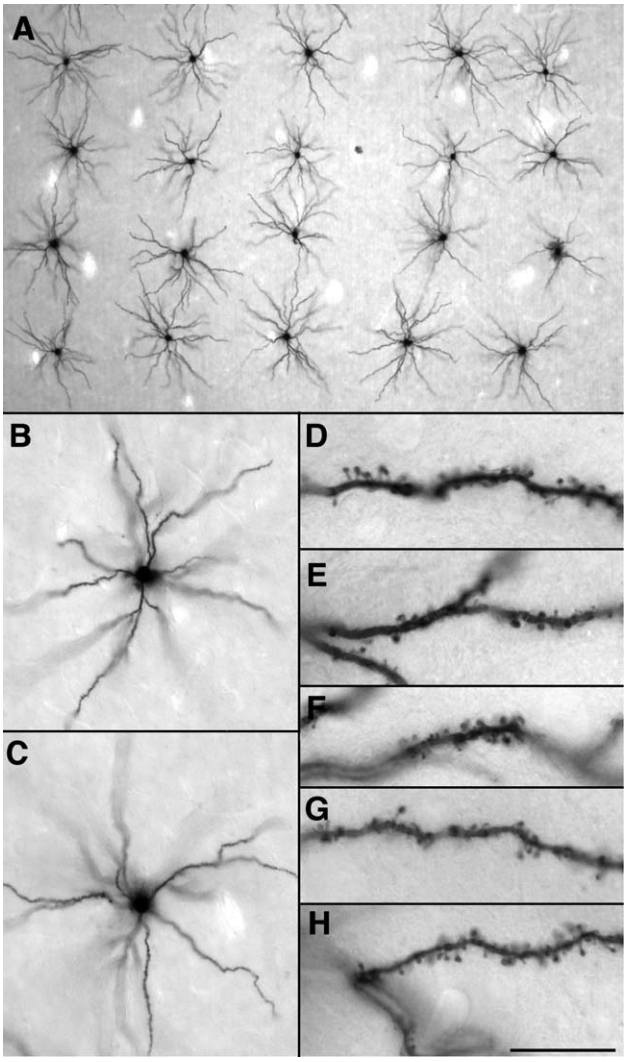

Fig. 1 – Photomicrographs of pyramidal cells that were injected with Lucifer Yellow and processed for a light-stable DAB reaction product. Cells were injected in tangential sections at the base of layer III. Neurones in the primary visual area (V1), the second visual area (V2) and the third visual area (V3) were included for analysis. Dendritic spines are easily visualized at high power. Note that the thickness of the dendrites, and the density of dendritic spines differ for cells in the different cortical areas. Scale bar = 400 μm in panel A, 100 μm in panels B and C and 20 μm in panels D–H.

2. Results

2.1. *Visual mapping experiments*

The results of a single experiment of multiunit receptive fields recordings in the visual cortex are illustrated in Fig. 2, in

which we have illustrated the receptive fields of neurons the were recorded along parallel mediolateral transects beginning in the primary visual area (V1) and extending toward the temporal pole. When the microelectrode was moved across the cortical surface, the multiunit receptive field moved in an orderly, continuous way through the visual field. As described previously (Picanço-Diniz et al., 1991), within V1 there is a point to point representation of the visual field where the lateral border represents the nasal border of the visual field, the rostral portion represents the lower field and the caudal region the upper field. Continuing along the transects beyond the lateral border of V1 revealed a second map of the visual space extending to the horizontal meridian, which we considered to be the lateral border of the second visual area (V2). Beyond the lateral border of V2 we found evidence for two different receptive field progressions, one in the caudal visual field extending towards the vertical meridian and one in the rostral visual field extending beyond the horizontal meridian into the lower visual field representation. While both the caudal and rostral fields may be part of a single complex, we have distinguished these two regions here into the third visual area (V3) and the antero-lateral area (AL). Extending beyond the lateral border of V3 receptive fields approach the temporal periphery again suggesting the presence of another visual area. We have tentatively named this visual area the posterior temporal area (TP). We conclude that the vertical meridian corresponds to V1/V2 border and the horizontal meridian represents the lateral border of V2. V3 and AL areas are placed laterally to V2. AL appears to be dedicated to the representation of the inferior visual field and V3 the superior visual field. It may be possible however that V3 and AL could be part of the same functional area as it has been proposed for V3 dorsal and V3 ventral in the monkey visual cortex. Both the V1/V2 border and the lateral V2 border were easily distinguished in our myelin and CO preparations (Fig. 3).

2.2. *Pyramidal cell morphology*

Three hundred and sixty-three layer III neurons were injected in cortical areas V1, V2 and V3 in two different animals. One hundred and ninety-seven of these cells were included for analyses as they had an unambiguous apical dendrite, were well filled, had their entire basal trees contained within the slice and were located at the base of layer III (77 in agouti 1 and 120 in agouti 3). Other cells that could not be unambiguously identified as pyramidal cells were not included for further analysis. Because of the unknown age of the animals and the difference in the size of their brains (20.5 gm and 17.6 gm, respectively) we present data for each individual case, according to the cortical visual areas in which they were located.

2.3. *Basal dendritic tree size*

In both cases the basal dendritic trees of layer III pyramidal cells were progressively larger through cortical areas V1, V2 and V3 (mean ± SEM: agouti 1, 12.58 ± 0.33 × 104 μm^2, 13.86 ± 0.64 × 104 μm^2 and 18.12 ± 0.44 × 104 μm^2, respectively; agouti 3, 10.90 ± 0.23 × 104 μm^2, 12.84 ± 0.44 × 104 μm^2 and 14.09 ± 0.35 × 104 μm^2, respectively) (Figs. 4 and 5, Table 1). One-way ANOVAs revealed these differences to be significant in both agouti 1 ($F_{(2)} = 48.6$, $P < 0.001$) and agouti 3 ($F_{(2)} = 32.0$, $P < 0.001$). *Post-hoc* analysis (Scheffe test) revealed 8 of all possible 12 pair-wise comparisons between cortical areas (within each case) to be significantly different.

2.4. *Complexity of the basal dendritic trees*

Plots of the results of Sholl analysis in which we counted the number of dendritic intersections in successive concentric circles with radii of 25 μm increments are shown in Figs. 4 and 5. Comparison of the Sholl data revealed that cells in V1 had fewer branches than those in V2. Cells in V3 of agouti 1 had more branches than those in V2. Cells in V3 of agouti 3 had a similar number of branches to those in V2. These trends were reflected in the peak branching complexity in V1, V2 and V3 of agouti 1 (mean ± SD: 16.29 ± 4.70, 24.36 ± 4.14, 30.94 ± 5.03, respectively) and agouti 3 (mean ± SD: 21.14 ± 3.17, 26.91 ± 5.56, 26.09 ± 4.95, respectively). Repeated measures ANOVAs revealed significant differences in the branching patterns of neurons in both agouti 1 ($F_{(1,\ 2)} = 36.04$) and agouti 3 ($F_{(1,\ 2)} = 20.78$). *Post-hoc* analysis revealed 8 of all possible 12 pair-wise comparisons between cortical areas (within each case) to be significantly different.

2.5. *Spine densities of the basal dendrites*

Over 10,000 individual spines were drawn and tallied. As reported previously (see Elston and DeFelipe, 2002 for a review), the spine density along the basal dendrites varied as a function of distance from the cell body to the distal tips. In agouti 1, the peak average spine density of cells in V1 (mean ± SEM: 11.8 ± 2.1) was less than that in V2 (14.8 ± 4.98) and V3 (13.2± 3.49). Likewise, in agouti 3, the peak average spine density of cells in V1 (12.6 ± 1.71) was less than that in V2 (13.17 ± 1.34) and V3 (17.7 ± 2.16) (Figs. 4 and 5). Repeated measures ANOVAs revealed the differences in spine density to be significant between cells in both agouti 1 ($F_{(1,\ 2)} = 3.84$, $P < 0.05$) and agouti 3. ($F_{(1,\ 2)} = 13.72$, $P < 0.05$). *Post-hoc* Scheffe tests revealed a significant difference between V1 and V2 in agouti 1 and between V3 vs. V1 and V2 in agouti 3. By combining data from the Sholl analyses and spine density counts we calculated the total number of dendritic spines in the basal dendritic tree of the "average" layer III pyramidal neuron. In both agouti 1 and agouti 3, cells in V1 (2623 and 2432, respectively) were less spinous than those in V2 (3916 and 4352, respectively), which were less spinous than those in V3 (4975 and 5163, respectively) (Fig. 6).

2.6. *Somal areas*

Cell bodies of pyramidal neurons became progressively larger with progression from V1 to V2 and V3 in both agouti 1 (mean ± SEM: 196.5 ± 3.84 μm^2, 199.6 ± 7.32 μm^2, 243.2 ± 5.68 μm^2, respectively) and agouti 3 (194.7 ± 2.60 μm^2,

209.9 ± 3.73μm^2, 217.2 ± 4.44 μm^2, respectively) (Figs. 4 and 5). Analyses of variance revealed these differences to be significant in both agouti 1 ($F_{(2)}$ = 24.86, P < 0.001) and agouti 3 ($F_{(2)}$ = 12.75, P < 0.001). *Post-hoc* analysis (Scheffe test) revealed 8 of all possible 12 between-area comparisons in the 2 animals to be significantly different (Table 2).

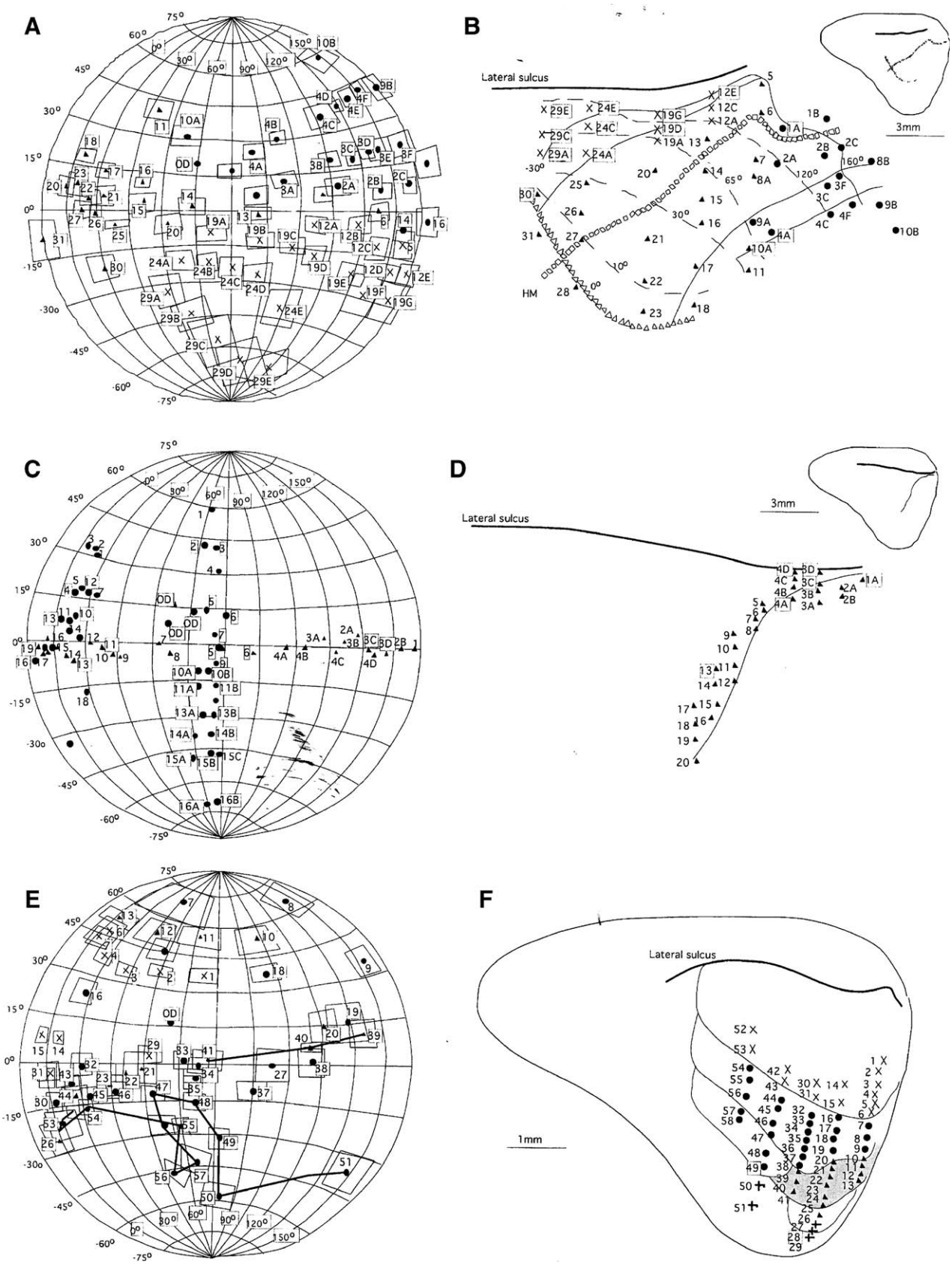

3. Discussion

Adult male agouties weigh up to 4–5 kg. The adult agouti brain weighs, on average, over seven times that of the adult rat brain, twenty-five times that of the adult mouse brain (Fig. 7). They are diurnal foragers, the young being born with their eyes open. Amongst the order Rodentia, they are relatively large species; however, they are not exceptional. The Paca (*Cuniculus paca*) weighs upwards of 15 kg, as does the Patagonian cavy (*Dolichotis salinicola*). The capybara (*Hydrochaeris hydrochaeris*), the largest of rodent species, weighs upwards of 80 kg (average 50 kg for males and 61 kg for females) (Nowak, 1999). Virtually nothing is known about the cortical microcircuitry of these large-brained rodent species—somewhat surprising given that the rat is the most commonly studied model of the larger human brain. Instead, most of what is known about the rodent cerebral cortex is restricted to studies of the rat and mouse, which represent a very small group within the order (Fig. 8).

3.1. *Organization of visual cortex*

Recent studies on the agouti reveal that it has a well-developed visual system adapted for its diurnal foraging habits (i.e., a diet of fruits, vegetables and succulent plants). Agoutis have relatively large, laterally positioned eyes with a prominent visual streak (Silveira, 1985; Picanço Diniz, 1987; Picanço-Diniz et al., 1989). By studying cytoarchitecture, myeloarchitecture, patterns of connectivity and receptive field properties, Picanço Diniz (1987); Picanço-Diniz et al. (1989) reported on the size and location of the primary visual area (V1). In addition, they described four distinctive architectonic fields lateral to V1 (Picanço-Diniz et al., 1989). In the present report we confirm and extend these findings by electrophysiological recordings, cytochrome oxidase histochemistry and myelin staining to include the second visual area (V2), the third visual area (V3), the anterolateral area (AL) and the posterior temporal area (TP). Collation of summary maps (Picanço Diniz, 1987) in which we reconstructed receptive fields of neurons across cases reveal a complete map of the visual space in a continuous belt immediately lateral to V1, bordered medially by the vertical meridian and laterally by the horizontal meridian. This continuous belt was also identifiable in sections processed for either myelin of CO, providing further evidence that this region of cortex corresponds to a single visual area, the second visual area. Such an interpretation is consistent with that reported in the diurnal species of suborder Hystrichomorpha (e.g., grey squirrel, Hall et al., 1971) but not in the nocturnal species (e.g., guinea pig, Choudhury, 1978) where there is evidence for a medial visual area nor species belonging to the suborder Myomorpha (Bravo et al., 1990; Espinoza and Thomas, 1992; Montero, 1993). Our estimations of the visual field representations lateral to V2 are more tentative but are in agreement with distinctive architectonic boundaries reported by Picanço-Diniz et al. (1989). Two different trends were observed in receptive field progressions extending lateral to V2. Thus, we have tentatively identified two cortical areas in this region, including the third visual area (V3) and the anterior lateral area (AL). However, for the purposes of quantifying pyramidal cell structure in striate and extrastriate visual areas in the

Fig. 2 – Schematic illustrating receptive fields of neurons recorded from visually responsive cortex in the agouti. Projections of individual receptive fields are mapped in both global space (A, C, E) and on the cortical surface (B, D, F) to illustrate topography in V1 (A, B), the horizontal meridian in V1 (C, D) and receptive field progressions along mediolateral transects from V1 into extrastriate cortex (E, F). When the microelectrode was moved across the cortical surface in V1, the multiunit receptive field moved in orderly, continuous way through the visual field (A–D). Note in V1 the lateral border represents the nasal border of the visual field, the rostral portion represents the lower field and the caudal region the upper field, as described previously (Picanço Diniz, 1987; Picanço-Diniz et al., 1991). Reversals in receptive field progressions were noted immediately lateral to the V1 lateral border when mapping along dorsolateral transects from striate to extrastriate cortex (E, F). In agreement with the myeloarchitecture and cytochrome oxidase (CO) staining we found evidence for a complete map of visual space in a continuous belt 1–2 mm wide immediately lateral to V1. Moreover, receptive fields in this belt were considerably larger than those noted at corresponding points in the visual field in V1 (e.g., compare points 1–6 in V1 [crosses] with points 7–9 [circles] in V2 in figures E and F). We name this region the second visual area (intermediate gray in F). Lateral progression beyond the lateral V2 border revealed another reversal in receptive fields about the horizontal meridian in agreement with the myeloarchitecture and CO staining. Receptive field progressions beyond the lateral V2 border revealed two different trends (E and F). In the caudal transects (e.g., points 10–13, 20–25 and 38–40) receptive fields approach the vertical meridian, whereas in the rostral transects (e.g., points 47–49 and 57–58) receptive fields progress into the lower visual field representation. Based on this and other cases we tentatively label these two regions as the third visual area (V3, shaded in dark gray in F) and the antero-lateral area (AL, shaded as white in F). Progression lateral to V3 reveals that receptive fields approach the temporal periphery in visual space (e.g., point 26) before becoming responsive to auditory stimulation. We tentatively name this most lateral visual area as the posterior temporal area (TP). We also found some neurons that were responsive to both visual and auditory stimuli (e.g., points 50, 51 and 52). According to this scheme the vertical meridian corresponds to V1/V2 border and the horizontal meridian represents the lateral border of V2. Areas V3 and AL are located immediately adjacent and lateral to V2. Area AL appears to be dedicated to the representation of the inferior visual field and V3 the superior visual field. The lateral margin of V3 corresponds with the vertical meridian. It may be possible however that V3 and AL could be part of the same functional area as it has been proposed for V3 dorsal and V3 ventral in the monkey visual cortex.

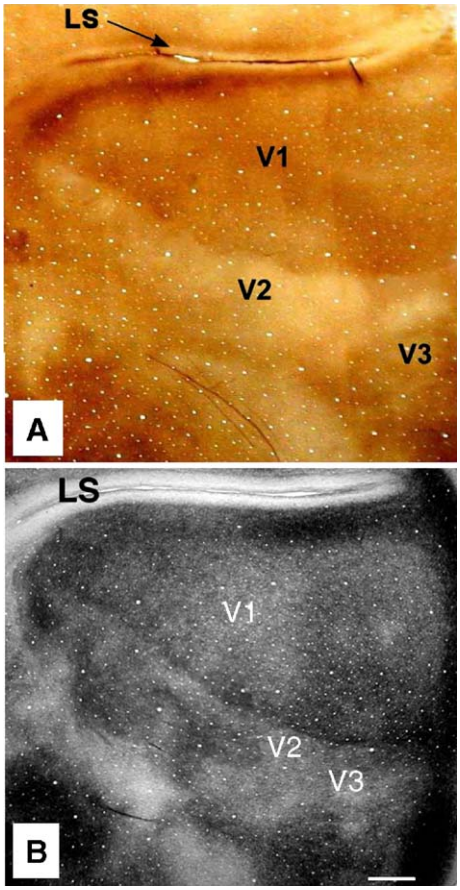

Fig. 3 – Photomicrograph of single sections obtained from a "flat-mount" preparation of the cerebral cortex that were processed for cytochrome oxidase (A) or myelin (B). Note the clearly distinguishable primary visual area (V1) adjacent to and extending inferior to the lateral sulcus (LS), the second visual area (V2) and the adjacent third visual area (V3). Scale bar = 2.0 mm.

Agouti we believe there are sufficient data to suggest that cells were injected in V1, V2 and immediately lateral to V2 (putative V3). Further experiments will be required to clarify the borders we propose between V3, AL and TP and shed light on the possibility that V3 and AL form part of a V3 complex (see Payne, 1993; Kaas, 1995, 1997, 2002; Rosa, 1997, 2002; Rosa and Krubitzer, 1999; Rosa and Manger, 2005; Krubitzer, 2000 for reviews).

3.2. *Pyramidal cell specializations in V1, V2 and V3*

Injection of supragranular pyramidal cells in V1, V2 and V3 revealed a clear trend for cells in increasing structural complexity with progression through these areas. More specifically, we found that cells in V1 are smaller and less spinous than those in V2, which were smaller and less spinous than those in the third visual area V3. Closer analysis revealed that cells in V1 had approximately half the number of spines in their basal dendritic trees compared to those in V3. This trend is consistent with that reported in a variety of species, including macaque, vervet, marmoset and owl monkeys, the baboon and the galago (Lund et al., 1993; Elston, 2003c; Elston et al., 1999a,b, 2005b,d,g), making it increasingly more likely that it is a general organizational principle in mammalian visual cortex. However, our studies in the Tree Shrew revealed a different trend, cells in V1 were more spinous than those in V2 (Elston et al., 2005f). Indeed, closer analyses reveals some interesting differences in the trends among species. For example, pyramidal cells in V1 of the agouti are larger, more branched and more spinous than those in primates, being approximately 4-fold more spinous than those in galagos, monkeys and baboons (Elston, 2003c; Elston and Rosa, 1997, 1998; Elston et al., 1999b, 2005b,d,g). Likewise, pyramidal cells in V2 of the agouti are more spinous than those in V2 of the above-mentioned primates, being, on average, 3–3.5 times more spinous. It is natural then to ask why layer III pyramidal cells in V1 and V2 of the agouti are so much more complex than their counterparts in homologous cortical areas in primates.

Studies in primates have revealed both scale variant and scale invariant specialization in pyramidal cell structure (Elston and Zietsch, 2005; Elston et al., 2001, 2006). That is, in some regions (e.g., granular prefrontal cortex) pyramidal cell structure is progressively more complex in successively larger brains whereas in other regions (e.g., V1) pyramidal cell structure is relatively uniform among species despite appreciable volumetric differences in the brain (e.g., Elston et al., 2006). These findings tend to suggest at least two principles act in concert to determine the pyramidal cell phenotype (and regional specializations thereof) in the normal adult brain: laws of form and species adaptations. The nature and scope of findings on pyramidal cell structure in non-primates (Elston et al., 1997; Dierssen et al., 2002; Benavides-Piccione et al., 2005, 2006; Ballesteros-Yáñez et al., 2006; present results) suggest that a possible third principal is at play—phylogenetic constraints. In simple terms, in the latter case evolutionary changes in pyramidal cell structure may be constrained within different phylogenetic levels (see Gould, 2002; Manger, 2005 for reviews). In other words, some aspect of brain evolution/development may be constrained in rodents but not primates (or vice versa) resulting in different expressions of the phenotype-manifest as different complexity in the dendritic trees of pyramidal cells. Clearly, more quantitative data are needed, particularly in non-primates, to provide the basis for a better understanding of the evolutionary and developmental influences on regional and species specializations in cortical microcircuitry.

Despite these considerable gaps in our understanding of the how and why of microstructural specialization in cortex of different species, there are compelling data on their potential functional implications (see Chklovskii et al., 2004; Treves, 2005; Jacobs and Scheibel, 2002; Elston, 2002, 2003, in press for reviews). Briefly, regional variation in pyramidal cell structure results in different numbers of inputs being sampled by individual neurons, differences in the degree of compartmentalization of processing these inputs within the dendritic trees, and different patterns of neuronal connectivity, which influence both cellular and systems function:

the more complex the structure the more complex the function. Accepting this to be the case, we can make some speculations about neuronal processing in visual cortex of the agouti in relation to that in tree shrews and primates. In both the agouti and the tree shrew, pyramidal cells in V1 are relatively spinous. In these same species pyramidal cells in inferotemporal cortex are more spinous than those in V1. However, the relative extent of these differences in the agouti and tree shrew is small by comparison to those in primates. For example, cells in V3 of the agouti are only

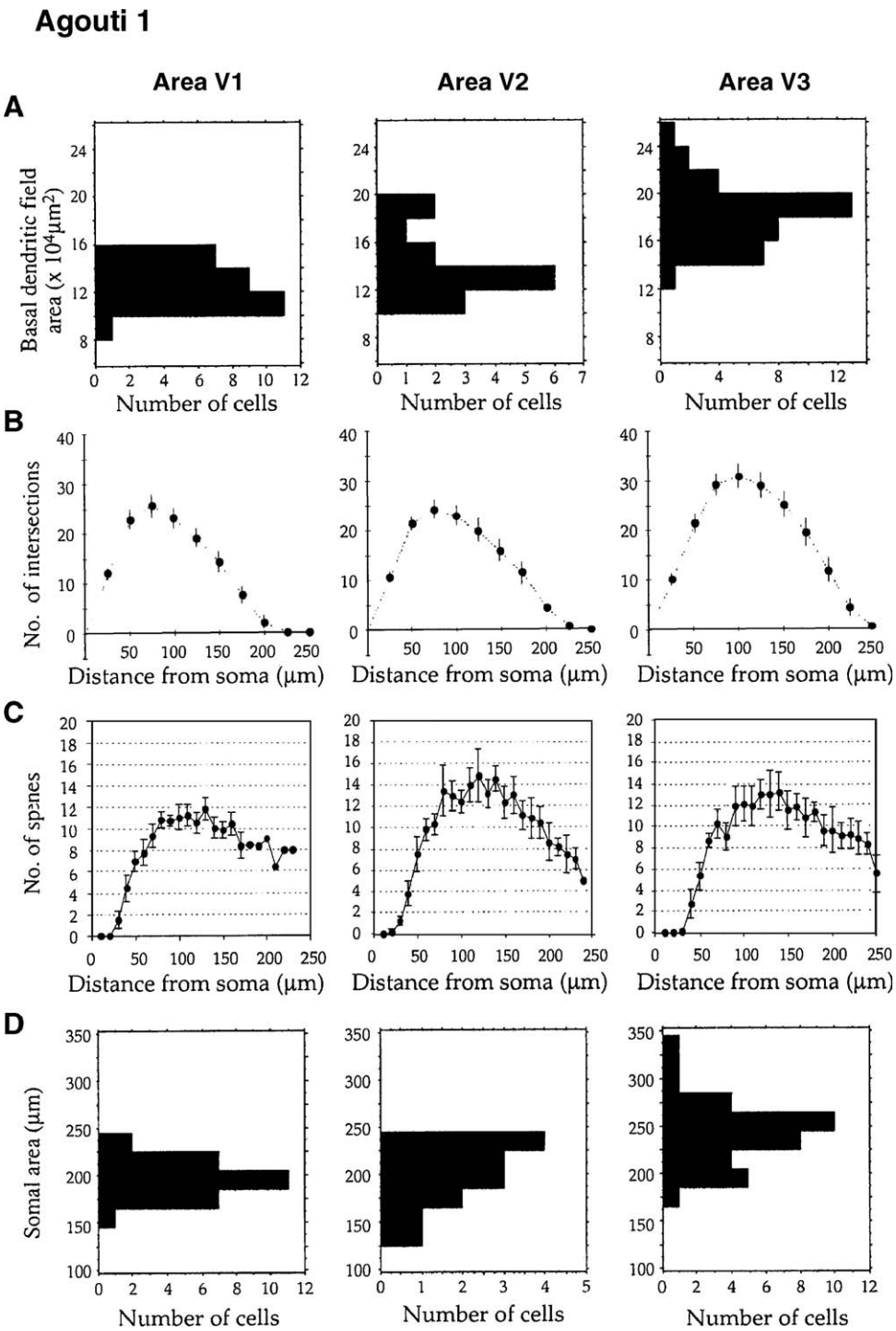

Fig. 4 – (A) Plots of the size of the basal dendritic trees of layer III pyramidal neurons sampled in the primary (V1), second (V2) and third (V3) visual areas in agouti 1. (B) Plots of the number of dendritic intersections of the basal dendrites of pyramidal neurons in V1, V2 and V3 in agouti 1. (C) Plots of the number of dendritic spines per 10 μm segment of dendrite, as a function of distance from the cell body, in the basal dendritic trees of layer III pyramidal neurons in V1, V2 and V3 in agouti 1. (D) Plots of the size of the somata of pyramidal neurons in V1, V2 and V3 of agouti 1.

2 times more spinous than those in V1. In the macaque monkey there is an 11-fold difference in the number of spines in the basal dendritic trees of cells in between V1 and inferotemporal cortex. The implication then is that there is lesser potential for an increase in functional complexity with progression through visual areas in the agouti by comparison with monkeys. Moreover, that cells in IT in the agouti and tree shrew perform less complex functions than their counterparts in monkeys. The reverse it true for cells in V1, those in the agouti and tree shrew

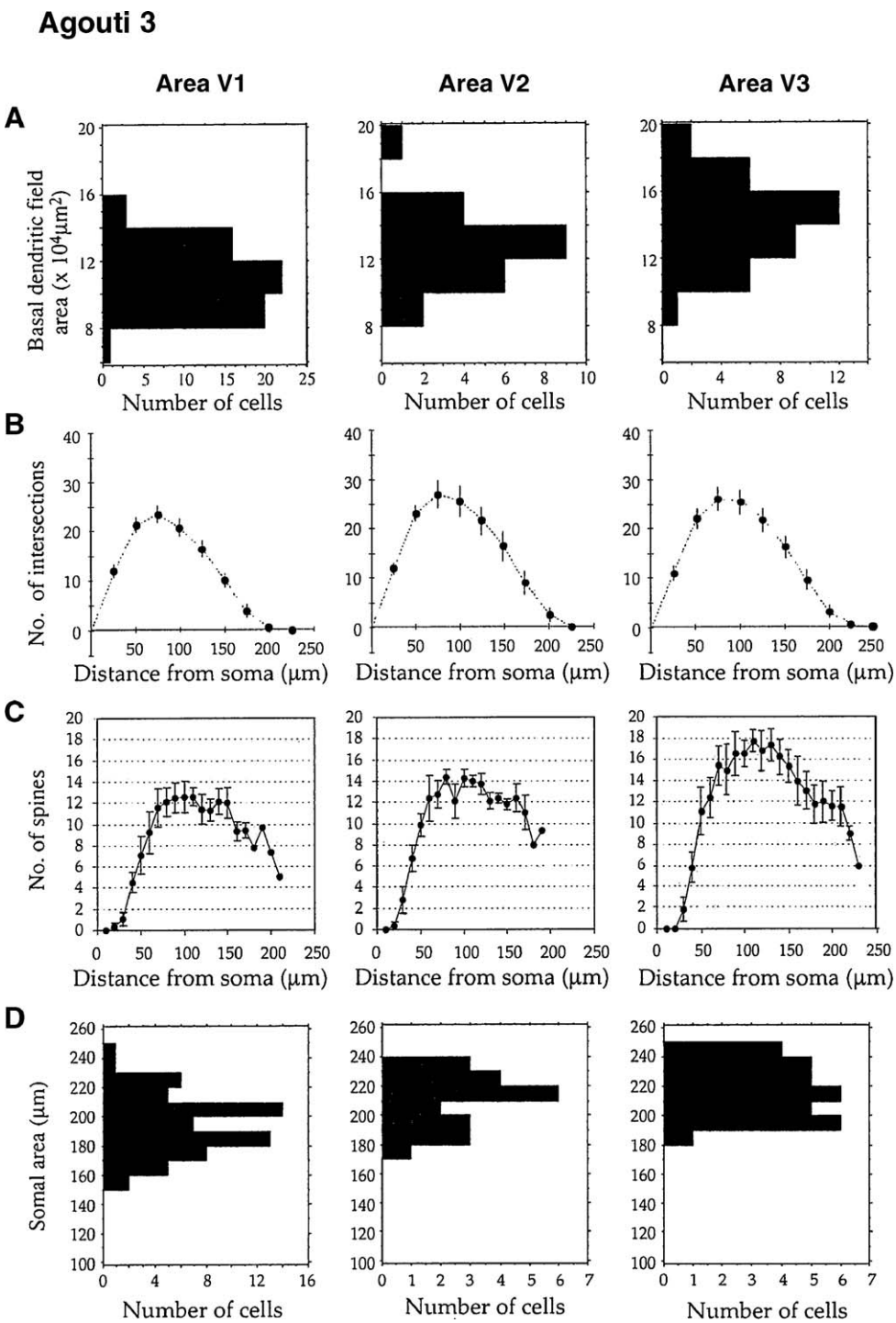

Fig. 5 – (A) Plots of the size of the basal dendritic trees of layer III pyramidal neurons sampled in the primary (V1), second (V2) and third (V3) visual areas in agouti 2. (B) Plots of the number of dendritic intersections of the basal dendrites of pyramidal neurons in V1, V2 and V3 in agouti 2. (C) Plots of the number of dendritic spines per 10 μm segment of dendrite, as a function of distance from the cell body, in the basal dendritic trees of layer III pyramidal neurons in V1, V2 and V3 in agouti 2. (D) Plots of the size of the somata of pyramidal neurons in V1, V2 and V3 of agouti 2.

Table 1 – Size of the basal dendritic trees (μm^2) of layer III pyramidal cells (case by case)

Visual area	n	Mean $\times 10^4$	SD $\times 10^4$	SEM $\times 10^4$	Minimum $\times 10^4$	Maximum $\times 10^4$
Agouti 1						
V1	28	12.58	1.76	0.33	9.46	15.49
V2	14	13.86	2.38	0.64	10.70	18.54
V3	35	18.12	2.61	0.44	13.19	24.83
Agouti 3						
V1	62	10.90	1.80	0.23	7.15	15.20
V2	22	12.84	2.06	0.44	8.38	18.07
V3	36	14.09	2.12	0.35	9.93	18.11

Table 2 – Size of the somata (μm^2) of layer III pyramidal cells (case by case)

Visual area	n	Mean	SD	SEM	Minimum	Maximum
Agouti 1						
V1	28	196.47	20.34	3.84	147.78	231.79
V2	14	199.56	27.39	7.32	141.28	232.63
V3	35	243.16	33.63	5.68	183.31	331.33
Agouti 3						
V1	62	194.72	20.49	2.60	154.38	247.12
V2	22	209.94	17.50	3.73	178.36	238.6
V3	36	217.22	26.66	4.44	109.84	254.23

potentially perform more complex function than their counterparts in primates.

4. Experimental procedures

4.1. *Electrophysiological mapping*

Many of the experimental procedures related to the visual recording have been described elsewhere (Picanço-Diniz et al., 1991). In brief 8 agoutis (*Dasyprocta primnolopha*, also known also as *D. leporine* or *D. aguti*) weighting 1.5–3.0 kg were used. The animals were anesthetized by intramuscular injections of a 1:4 mixture of 2% tiazine chloridrate (Rompun, Bayer) and 5% ketamine chloridrate (Ketalar, Parke-Davis). A stable anesthetic level was obtained using 1 ml of the mixture/kg of body weight at 2 h intervals. The electrocardiogram and electroencephalogram were recorded throughout the experiment and used to monitor the anesthetic level. Additional doses of anesthetic were given when necessary. Body core temperature was maintained at 37 °C. A tracheotomy was performed and the animal ventilated artificially. A craniotomy was performed, the dura mater was reflected and the exposed cortical surface protected with warm mineral oil.

The animals were secured in a headholder especially designed to minimize obstruction of the visual field for species with laterally positioned eyes (Silva-Filho et al., 1991). The eye was aligned with reference to an oculocentric equatorial azimuthal coordinate system. In these system the vertical meridian roughly corresponded to the nasotemporal retinal decussation and the horizontal meridian corresponds to the visual streak (Silveira et al., 1989). Cycloplegia and mydriasis were obtained with 1% atropine

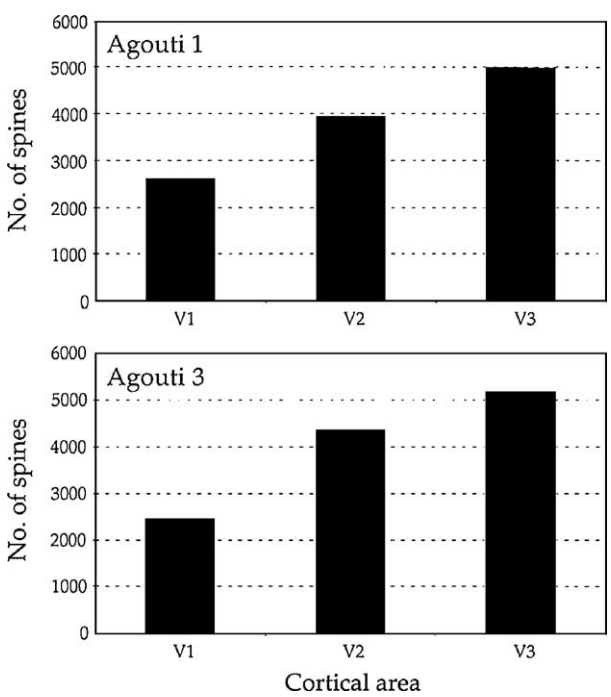

Fig. 6 – Plots of our estimates of the total number of spines in the dendritic tree of the "average" layer III pyramidal cells in the primary (V1), second (V2) and third (V3) visual areas of the agouti. Note the systematic increase in the number of spines with lateral progression through these cortical areas in both agouti 1 and agouti 3.

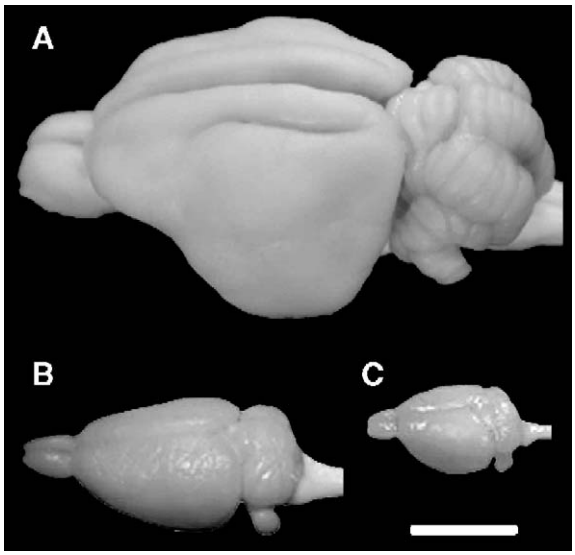

Fig. 7 – Photomicrograph of the dorso-lateral aspect of the brain of the agouti, rat and mouse. Note the difference in size, and the presence of a clearly identifiable lateral sulcus in the agouti not present in the rat or mouse. Scale bar = 10.0 mm.

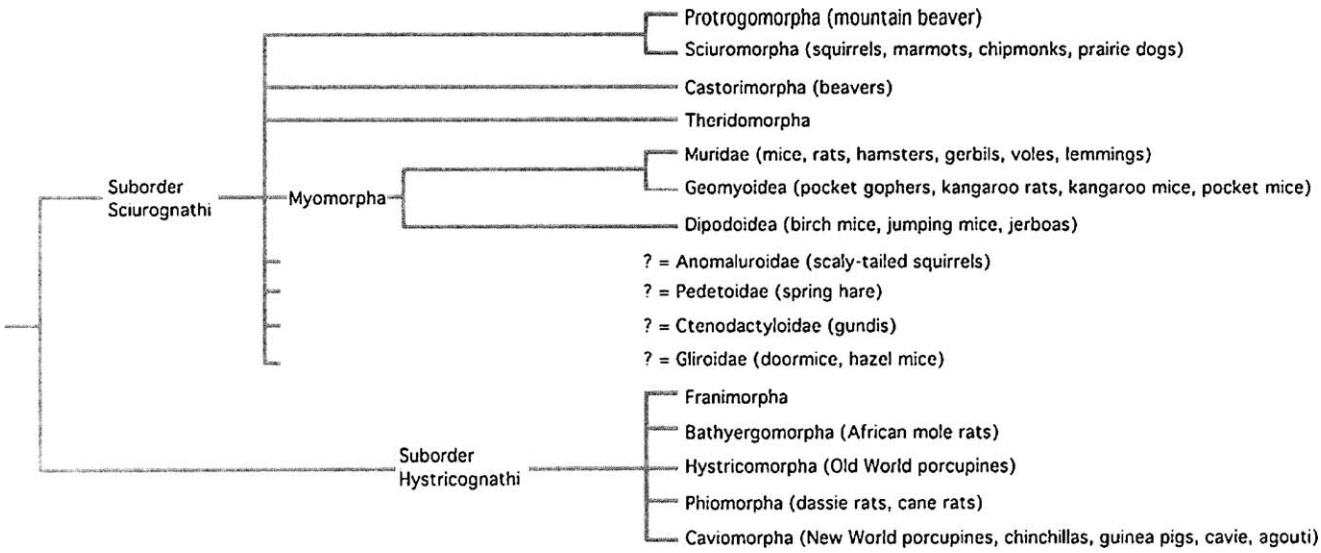

Fig. 8 – Figure illustrating the phylogenetic tree of the order Rodentia, including selected species of the Caviomorpha characterized by large body mass such as the agouti (*Dasyprocta primnolopha*, also known as *D. aguti*), the Patagonian cavy, the Paca and the Capybara.

sulfate applied to the eyes. The cornea was protected with a thin layer of silicone fluid (Dow Corning 200/350). The projection of the optic disk in the visual field was checked throughout the experiment by means of a reversible ophthalmoscope. For visual experiments the activity of small clusters of neurons was recorded by varnish insulated tungsten microelectrodes positioned in a micromanipulator. The signal was amplified in a differential amplifier and fed to a dual-beam storage oscilloscope and to an audio monitor system. Visual stimulation was carried out using hand-held cards drifted tangential to the hemisphere.

At the end of the experiment the animals were perfused through the aorta with warm 0.9% saline solution followed by aldehyde fixatives (4% paraformaldehyde in 0.1 M phosphate buffer pH 7.2–7.4 or 10% formaldehyde-saline solution). The brains were removed from the skull and processed for microscopic analysis. Coronal serial sections, 50 μm thick, were mounted and stained by the methods of Nissl and Gallyas (Gallyas, 1979). Alternatively the hemispheres were dissected from the rest of the subcortical structures and then flattened overnight between glass slides and cut tangentially on vibratome. Reactions for alternate sections for myelin and cytochrome-oxidase were as reported elsewhere (Gallyas, 1979; Wong-Riley, 1979 respectively) lightly modified. Identification of recording sites was performed by searching for the microelectrode tracts and electrolytic lesions made during the recordings. We used bi-dimensional reconstruction of the flattened cortical surface using anatomical landmarks to superimpose different sections of the same or different subjects. The reconstruction was done as follows: first, we prepared an enlarged view of each coronal section using a photographic enlarger, then we chose the fundus of the lateral sulcus, which corresponds to the medial border of area 17 (Picanço-Diniz et al., 1991), as a reference point. A digitizing table was then used to measure the lateral position of each penetration in relation to the fundus of the lateral sulcus by generating a flat reconstruction of the visual recording sites.

4.2. *Intracellular injection*

An additional two adult male agouti (3.9 and 2.4 kg) were anesthetized by i.m. injection of 1:4 ketamine rompun (1 ml/kg) and overdosed by intracardial injection of pentobarbitone. Following transcardial perfusion (0.95% saline in 0.1 M phosphate buffer {PB; pH 7.2} followed by 4% paraformaldehyde in PB) the brains were removed, the right hemispheres were flat-mounted (see Elston and Rosa, 1997 for details). The next day serial 250 μm sections were cut with the aid of a Vibratome, prelabeled with 10^{-5} mol/L 4,6 diamidino-2-phenylindole (D9542, Sigma, USA) and mounted into a perspecx chamber on a fixed stage fluorescence microscope (Zeiss Axioskop II FS). Cells were injected under visual control with Lucifer Yellow (LY; L-0259, Sigma: 8% in 0.1 M Tris buffer, pH 7.4) by continuous negative current. Following cell injection the sections were processed with an antibody raised against-LY (provided by Prof. DeFelipe) (1:400 000 in a solution containing 2% bovine serum albumin {Sigma A3425}, 1% Triton X-100 {BDH 30632}, 5% sucrose in 0.1 mol/l phosphate buffer) for 5 days at room temperature. Standard immunohistochemical procedures were then used to reveal cell structure, using 3,3′-diaminobenzidine (DAB; Sigma D 8001) as the chromogen (Fig. 1) (see Elston et al., 1997 for details).

Cells were drawn with the aid of a Zeiss Axioplan equipped with a camera lucida, and further analyzed in 2-dimensions. Dendritic tree size (the area contained within a polygon joining the outermost distal tips of the basal dendrites) and somal size were determined with the aid of NIH-Image software (NIH, Bethesda, US) (e.g. Elston and Rosa, 1997). Branching patterns were determined by Sholl analysis (e.g., Sholl, 1953). Spine density was determined per 10 μm of dendrite as a function of distance from the cell body to the

distal tips of the dendrites (Eayrs and Goodhead, 1959; Valverde 1967). The total number of spines found in the basal dendritic tree of the "average" pyramidal cell in each cortical area was calculated by multiplying the average number of spines of a given portion of dendrite by the average number of branches for the corresponding region, over the entire dendritic tree (Elston, 2001). All statistical analyses were performed with SPSS (SPSS Inc. IL, USA).

Acknowledgments

Thanks go to Jean-Christophe Houzel for help in obtaining animals and initiating the collaboration. Thanks also to Laura Ferris and Brendan Zeitsch for technical help. Supported by grants from the JS McDonnell Foundation, the Australian National Health and Medical Research Council and the National Research Council-CNPq and FINEP of Brazil.

REFERENCES

Ballesteros-Yáñez, I., Benavides-Piccione, R., Elston, G.N., Yuste, R., DeFelipe, J., 2006. Density and morphology of pyramidal cell dendritic spines in the mouse neocortex. Neuroscience 138, 403–409.

Benavides-Piccione, R., Dierssen, M., Ballesteros-Yanez, I., Arbonés, M., Fotaki, V., DeFelipe, J., Elston, G.N., 2005. Alterations in the phenotype of neocortical pyramidal cells in the Dyrk1A+/– mouse. Neurobiol. Dis. 20, 115–122.

Benavides-Piccione, R., Hamzei-Sichani, F., Ballesteros-Yanez, I., Defelipe, J., Yuste, R., 2006. Dendritic size of pyramidal neurons differs among mouse cortical regions. Cereb. Cortex. 16, 990–1001.

Bravo, H., Olavarria, J., Torrealba, F., 1990. Comparative study of visual inter and intrahemispheric cortico-cortical connections in five native Chilean rodents. Anat. Embryol. (Berl.) 181, 67–73.

Chklovskii, D.B., Mel, B.W., Svoboda, K., 2004. Cortical rewiring and information storage. Nature 431, 782–788.

Choudhury, B.P., 1978. Retinotopic organization of the guinea pig's visual cortex. Brain Res. 144, 19–29.

Dierssen, M., Benavides-Piccione, R., Martínez-Cué, C., Estivill, X., Flórez, J., Elston, G.N., DeFelipe, J., 2002. Alterations of neocortical pyramidal cell phenotype in the TS65Dn mouse model of Down syndrome: effects of environmental enrichment. Cereb. Cortex 13, 758–764.

Eayrs, J.T., Goodhead, B., 1959. Postnatal development of the cerebral cortex in the rat. J. Anat. 93, 385–402.

Elston, G.N., 2001. Interlaminar differences in the pyramidal cell phenotype in cortical areas 7m and STP (the superior temporal polysensory area) of the macaque monkey. Exp. Brain Res. 138, 141–152.

Elston, G.N., 2002. Cortical heterogeneity: implications for visual processing and polysensory integration. J. Neurocytol. 31, 317–335.

Elston, G.N., 2003a. Comparative studies of pyramidal neurons in visual cortex of monkeys. In: Kaas, J.H., Collins, C. (Eds.), The Primate Visual System. CRC Press, Boca Raton, pp. 365–385.

Elston, G.N., 2003b. Cortex, cognition and the cell: new insights into the pyramidal neuron and prefrontal function. Cereb. Cortex 13, 1124–1138.

Elston, G.N., 2003c. Pyramidal cell heterogeneity in the visual cortex of the nocturnal New World owl monkey (*Aotus trivirgatus*). Neuroscience 117, 213–219.

Elston, G.N., in press. Specializations in pyramidal cell structure during primate evolution. In: Kaas, J.H., Preuss, T., M. (eds) Evolution of Nervous Systems, vol 5. Elsevier, Oxford.

Elston, G.N., DeFelipe, J., 2002. Spine distribution in neocortical pyramidal cells: a common organizational principle across species. In: Azmitia, E.C., DeFelipe, J., Jones, E.G., Rakic, P., Ribak, C.E. (Eds.), Prog. Brain. Res., vol. 136. Elsevier, pp. 109–133.

Elston, G.N., Rockland, K., 2002. The pyramidal cell of the sensorimotor cortex of the macaque monkey: phenotypic variation. Cereb. Cortex 10, 1071–1078.

Elston, G.N., Rosa, M.G.P., 1997. The occipitoparietal pathway of the macaque monkey: comparison of pyramidal cell morphology in layer III of functionally related cortical visual areas. Cereb. Cortex 7, 432–452.

Elston, G.N., Rosa, M.G.P., 1998. Morphological variation of layer III pyramidal neurones in the occipitotemporal pathway of the macaque monkey visual cortex. Cereb. Cortex 8, 278–294.

Elston, G.N., Rosa, M.G.P., in press. Ipsilateral corticocortical projections to the primary and middle temporal visual areas of the primate cerebral cortex: area-specific variations in the morphology of connectionally identified pyramidal cells. Eur. J. Neurosci.

Elston, G.N., Zietsch, B., 2005. Fractal analysis as a tool for studying specialization in neuronal circuitry: the study of the evolution of the primate cerebral cortex and human intellect. Adv. Complex Systems 8, 217–227.

Elston, G.N., Pow, D.V., Calford, M.B., 1997. Neuronal composition and morphology in layer IV of two vibrissal barrel subfields of rat cortex. Cereb. Cortex 7, 422–431.

Elston, G.N., Tweedale, R., Rosa, M.G.P., 1999a. Cortical integration in the visual system of the macaque monkey: large scale morphological differences of pyramidal neurones in the occipital, parietal and temporal lobes. Proc. R. Soc. London, Ser. B 266, 1367–1374.

Elston, G.N., Tweedale, R., Rosa, M.G.P., 1999b. Cellular heterogeneity in cerebral cortex. A study of the morphology of pyramidal neurones in visual areas of the marmoset monkey. J. Comp. Neurol. 415, 33–51.

Elston, G.N., Benavides-Piccione, R., DeFelipe, J., 2001. The pyramidal cell in cognition: a comparative study in human and monkey. J. Neurosci. 21, RC163.

Elston, G.N., Benavides-Piccione, R., DeFelipe, J., 2005a. A study of pyramidal cell structure in the cingulate cortex of the macaque monkey with comparative notes on inferotemporal and primary visual cortex. Cereb. Cortex 15, 64–73.

Elston, G.N., Benavides-Piccione, R., Elston, A., DeFelipe, J., Manger, P., 2005b. Pyramidal cell specialization in the occipitotemporal cortex of the Chacma baboon (*Papio ursinus*). Exp. Brain Res. 167, 496–503.

Elston, G.N., Benavides-Piccione, R., Elston, A., DeFelipe, J., Manger, P., 2005c. Specialization in pyramidal cell structure in the sensory-motor cortex of the vervet monkey (*Cercopithecus pygerythrus*). Neuroscience 134, 1057–1068.

Elston, G.N., Benavides-Piccione, R., Elston, A., Manger, P., DeFelipe, J., 2005d. Pyramidal cell specialization in the occipitotemporal cortex of the vervet monkey (*Cercopithecus pygerythrus*). NeuroReport 16, 967–970.

Elston, G.N., Benavides-Piccione, R., Elston, A., Manger, P., DeFelipe, J., 2005e. Specialization in pyramidal cell structure in the sensory-motor cortex of the Chacma baboon (*Papio ursinus*) with comparative notes on the macaque monkey. Anat. Rec. 286A, 854–865.

Elston, G.N., Elston, A., Casagrande, V.A., Kaas, J., 2005f. Areal specialization in pyramidal cell structure in the visual cortex of the tree shrew: a new twist revealed in the evolution of cortical circuitry. Exp. Brain Res. 163, 13–20.

Elston, G.N., Elston, A., Kaas, J., Casagrande, V.A., 2005g. Regional specialization in pyramidal cell structure in the visual cortex of the galago. An intracellular injection study with comparative notes on New World and Old World monkeys. Brain Behav. Evol. 66, 10–21.

Elston, G.N., Benavides-Piccione, R., Elston, A., Zietsch, B., DeFelipe, J., Manger, P., Casagrande, V., Kaas, J.H., 2006. Specializations of the granular prefrontal cortex of primates: implications for cognitive processing. Anat. Rec. 288A, 26–35.

Espinoza, S.G., Subiabre, J.E., Thomas, H.C., 1992. Retinotopic organization of striate and extrastriate visual cortex in the golden hamster (*Mesocricetus auratus*). Biol. Res. 25, 101–107.

Gallyas, F., 1979. Silver staining of myelin by means of physical development. Neurol. Res. 1, 203–209.

Gould, S.J., 2002. The Structure of Evolutionary Theory. Harvard Univ. Press, Cambridge, MA.

Hall, W.C., Kaas, J.H., Killackey, H., Diamond, I.T., 1971. Cortical visual areas in the grey squirrel (*Sciurus carolinesis*): a correlation between cortical evoked potential maps and architectonic subdivisions. J. Neurophysiol. 34, 437–452.

Jacobs, B., Scheibel, A.B., 2002. Regional dendritic variation in primate cortical pyramidal cells. In: Schüz, A., Miller, R. (Eds.), Cortical Areas: Unity And Diversity. Taylor and Francis, London, pp. 111–131.

Jacobs, B., Schall, M., Prather, M., Kapler, L., Driscoll, L., Baca, S., Jacobs, J., Ford, K., Wainwright, M., Treml, M., 2001. Regional dendritic and spine variation in human cerebral cortex: a quantitative study. Cereb. Cortex 11, 558–571.

Kaas, J.H., 1995. The evolution of isocortex. Brain Behav. Evol. 46, 187–196.

Kaas, J.H., 1997. Theories of visual cortex organization in primates. In: Rockland, K., Kaas, J.H., Peters, A. (Eds.), Extrastriate Cortex in Primates, vol 12. Cereb. Cortex, vol. 12. Plenum, New York, pp. 91–125.

Kaas, J.H., 2002. Neocortex. Encyclopaedia of the Human Brain, vol. 3, pp. 291–303.

Krubitzer, L.A., 2000. How does evolution build a complex brain. In: Bock, G.R., Cardew, G. (Eds.), Evolutionary Developmental Biology of the Cerebral Cortex. Wiley, Chichester, pp. 206–226.

Lund, J.S., Yoshioka, T., Levitt, J.B., 1993. Comparison of intrinsic connectivity in different areas of macaque monkey cerebral cortex. Cereb. Cortex 3, 148–162.

Manger, P.R., 2005. Establishing order at the systems level in mammalian brain evolution. Brain Res. Bull. 66, 282–289.

Montero, V.M., 1993. Retinotopy of cortical connections between the striate cortex and extrastriate visual areas in the rat. Exp. Brain Res. 94, 1–15.

Nowak, R.M., 1999. Walker's mammals of the World. Johns Hopkins Univ. Press, Baltimore.

Payne, B.R., 1993. Evidence for visual cortical area homologs in cat and macaque monkey. Cereb. Cortex 3, 1–5.

Picanço Diniz, C.W., 1987. Organizaçáo do sistema visual de roedores da amazônia: topografia das áreas corticais visuais da cutia, Dasyprocta aguti. PhD thesis Universidade Federal do Rio de Janeiro.

Picanço-Diniz, C.W., Oliveira, H.L., Silveira, L.C., Oswaldo-Cruz, E., 1989. The visual cortex of the agouti (*Dasyprocta aguti*): architectonic subdivisions. Braz. J. Med. Biol. Res. 22, 121–138.

Picanço-Diniz, C.W., Silveira, L.C.L., De Carvalho, M.S.P., Oswaldo-Cruz, E., 1991. Contralateral visual field representation in area 17 of the cerebral cortex of the agouti: a comparison between the cortical magnification factor and the retinal ganglion cell distribution. Neuroscience 44, 325–333.

Rosa, M.G.P., 1997. Visuotopic organization of primate extrastriate cortex. In: Rockland, K., Kaas, J.H., Peters, A. (Eds.), Extrastriate Cortex in Primates, vol 12. Cerebral Cortex, vol. 12. Plenum, New York, pp. 127–204.

Rosa, M.G.P., 2002. Visual maps in the adult primate cerebral cortex; some implications for brain development and evolution. Braz. J. Med. Biol. Res. 35, 1485–1498.

Rosa, M.G.P., Krubitzer, L.A., 1999. The evolution of visual cortex: where is V2? Trends Neurosci. 22, 242–248.

Rosa, M.G.P., Manger, P.R., 2005. Clarifying homologies in the mammalian cerebral cortex: the case of the third visual area (V3). Clin. Exp. Pharmacol. Physiol. 32, 327–339.

Sereno, M.I., McDonald, C.T., Allman, J.M., 1994. Analysis of retinotopic maps in extrastriate cortex. Cereb. Cortex 4, 601–620.

Sholl, D.A., 1953. Dendritic organization in the neurons of the visual and motor cortices of the cat. J. Anat. 87, 387–406.

Silva-Filho, M., Picanço Diniz, C.W., Oswaldo-Cruz, E., 1991. Head holder for lateral-eyed species in vision research. Braz. J. Med. Biol. Res. 24, 717–719.

Silveira, L.C.L., 1985. Organizaçáo do sistema visual de roedores da amazônia: Óptica Ocular e Distribuição das Células Ganglionares Retinianas. PhD thesis, Universidade Federal do Rio de Janeiro.

Silveira, L.C.L., Picanco-Diniz, C.W., Sampaio, L.F.S., Oswaldo-Cruz, E., 1989. Retinal ganglion cell distribution in the Cebus monkey: a comparison with the cortical magnification factors. Vision Res. 29, 1471–1483.

Treves, A., 2005. Frontal latching networks: a possible neural basis for infinite recursion. Cogn. Neuropsychol. 22, 276–291.

Valverde, F., 1967. Apical dendritic spines of the visual cortex and light deprivation in the mouse. Exp. Brain Res. 3, 337–352.

Wong-Riley, M., 1979. Changes in the visual system of monocularly sutured or enucleated cats demonstrable with cytochrome oxidase histochemistry. Brain Res. 171, 11–28.